Transition to time-dependent free convection in an inclined air layer

J. F. Pignatel and J. F. Marcillat*

The steadiness of free convection flow of air inside a rectangular tilted enclosure was investigated. The transition from a stationary to a non-stationary state was detected by measurement of the temperature within the air. The transition thresholds were plotted with respect to the Rayleigh number, the tilt angle and the aspect ratio. For the horizontal situation the results are in good agreement with previous data, but for tilted situation the lack of previous data makes valid comparisons difficult.

Keywords: *free convection flow, air flow, time-dependent flow, inclined fluid layer, tilted cavity, turbulence, transition threshold*

Introduction

The main initial purpose of this work was the evaluation of the heat losses of a flat-plate solar collector working at a 'mean temperature' in the range 0°C to 120°C. Such a collector was first considered with a view to realizing small distributed thermal power stations by using selective absorbing plates. But it appeared, in measuring heat transfer in a simulating model, that it was strongly dependent on the stationary or non-stationary nature of the internal free convection flow, so that the problem required particular study of the onset of time dependence of the flow.

Review of previous work

Free convection motion in a tilted fluid layer heated from one side has received considerable attention in an attempt to explain the development of turbulence from a static state by way of different transitions. The onset of the time dependence of such convective flows plays a special role in the occurrence of turbulent motion since it takes different forms according to the values of the fundamental parameters: Rayleigh number, aspect ratio and tilt angle. In addition the onset of time dependence and, more so, the onset of turbulence usually result in an increase in hear transfer, so that this increase has been used[1] as a criterion for the transition. The limits of the steady flow conditions in terms of the three parameters in an inclined layer are not well defined, so they were the major motivation for the experimental investigation reported here.

The particular cases of horizontal or vertcial low Prandtl number fluid layers have received more attention from an experimental and theoretical point of view. In the more general case when the fluid layer is inclined, convection assumes the form of longitudinal rolls aligned with the direction of inclination. The tilted layer is in general subject to two types of instability: the static top-heavy type of instability associated with the horizontal case, and the dynamic type which applies in the vertical case. At small angles of inclination the former type comes into play first, whereas at tilt angles near the vertical position the latter type is preponderant.

The transition to time-dependent convection in a horizontal fluid layer has been studied experimentally[1-3] and theoretically[4-7]; these studies have revealed the strong effect of the wave number associated with the Rayleigh number.

When the fluid layer is vertical, the motion exists for any finite Rayleigh number. However, provided this parameter is sufficiently small, the motion consists of on large single cell, the fluid rising on the hot wall, falling down the cold wall and turning at the opposite ends of the cavity. This flow, usually called 'base flow', was first described by Batchelor[8], who showed that the heat transfer from one vertical wall to the other is mainly by conduction. For sufficiently large values of Ra, the vertical motion is confined mainly to boundary layers on the two vertical walls, and in that case the dominant mode of transfer is convection. The temperature distribution and flow pattern predicted have been confirmed experimentally[9-11] and these motions have been the subject of further studies from analytical and numerical points of view[12-17]. Attempting to obtain an experimental visualization of the boundary layer oil flows which precede and follow the onset of convective turbulence, Elder[11] has discovered secondary stationary motions as transverse horizontal rolls in the interior of the slot, which were able to generate other steady secondary flows, to be called tertiary flows. These results have been confirmed by Vest and Arpaci[18] with experiments at $Pr = 1000$ which exhibited, in addition, secondary motion in an air-filled cavity ($Pr = 0.71$) for the conduction regime, giving an experimental corroboration of the results of Gershuni[19], who applied the linear stability theory to this regime and obtained highly approximate curves of neutral stability for the case of stationary disturbances. The stability characteristics of the flow in the conduction regime can be considered to be well established owing to

* Institut de Mecanique des Fluides de Marseille, 1 rue Honnorat, 13003 Marseille, France
Manuscript received 8 July 1985 and accepted for publication on 19 December 1985

the work of several investigators[18,20-28]. The main result of these analyses is that the type of instability is determined by the magnitude of the Prandtl number: the critical disturbance modes are steady when $Pr < 12.7$, but they are travelling waves when $Pr > 12.7$.

With respect to the boundary layer regime, the stability analysis has been first carried out for specialized conditions or for restricted ranges of the governing parameters[18,29-33]. For Prandtl number ranging from 0.73 to 1000, Bergholz[34] performed stability computations over a large interval in magnitude of the stratification parameter γ related to the vertical gradient in the cavity. At both low and high Pr, a change in the mode instability occurs if the vertical stratification is increased beyond a certain level; for $0.73 < Pr < 12.7$ there is a transition from stationary to travelling-wave instability if γ exceeds a certain magnitude depending upon the Pr value. However, if the Prandtl number is larger than 12.7, the transition with increasing γ is from travelling-wave to stationary instability. More recently, Roux and coworkers[35,36] determined numerically the minimum critical calue of Rayleigh number for the appearance of such two-dimensional stationary disturbances in an air-filled cavity, and the critical Ra value at which a reverse transition to monocellular motion occurs.

All these studies concern the two-dimensional character and stationary state of the motion, whereas very few investigations were devoted to three-dimensional and/or unsteady convective flows, with regard to the limitations imposed by physical experimentation and available techniques of numerical or mathematical analysis. Mallinson and de Vahl Davis[37] investigated three-dimensional natural convection in a box from a numerical point of view, and Elder[38] studied the turbulent free convection in a vertical slot from an experimental point of view.

When a fluid layer confined in a parellelepiped enclosure is inclined, the different types of instability are present and mixed, and are complicated by three-dimensionality and time-dependence effects. Some types of instability were identified by Hart[39,40], who concluded that the transition to wavy vortices is crucial to the development of violent unsteadiness. At some intermediate tilt angle $\alpha_{c,r}$ there is a cross-over from one class of instability to the other: the instability is roll-like, with axis in the X-direction for $\alpha < \alpha_{c,r}$ and in the Z-direction for $\alpha > \alpha_{c,r}$. The critical value $\alpha_{c,r}$ is a strong function of the fluid nature (Prandtl number) but also of the aspect ratio. For large l values the critical value is close to 70° for zir ($Pr = 0.71$) and to 90° for fluids having higher Pr values[39-44]. For $\alpha < \alpha_{c,r}$ the stationary longitudinal instability is characterized by a critical Rayleigh number independent of Pr and given by $Ra_{c,r} \cos\alpha = 1708$. For $\alpha > \alpha_{c,r}$ the transversal instability changes from rolls with axis in the Z-direction for small Pr values to wavy vortices for higher Pr values; the critical Rayleigh number increases with Pr but depends only slightly on the tilt angle. It seems[45] that this critical value of α is characterized by the minimum value of Nusselt number as a function of α. Arnold *et al*[46] have shown that $\alpha_{c,r}$ at the minimum value of Nu decreases with the aspect ratio up to $l \approx 12$ and then goes to an asymptotic value close to 70°.

The development of unsteadiness in the convective flows has received relatively little attention. The calculations of Clever and Busse[47] concerned the oscillatory instability for small tilt angles from 0° to 20°. From an experimental point of view, Schinkel[3] has studied that transition but for small values of the aspect ratio. An interesting review of the literature devoted to this problem followed by suggestions for interpretation of some observations has been carried out by Azouni[48] with particular attention to crystal growth problems.

The lack of data about this important question provided the challenge for the work described in this paper.

Experimental apparatus and procedure

The present experiments were carried out in a rectangular cavity specially adapted to temperature measurement and flow visualization with respect to the thickness, the inclination, the temperature level and the aspect ratio of the cavity.

Fig 1 shows a sectional view of the apparatus; it consisted of a 6 mm thick copper plate 0.80 m by 0.80 m heated from below by 10 electric strip-heaters and maintained at a uniform temperature by adjusting the electrical input to the heaters through a temperature regulator. To reduce the heat transferred from the hot plate to the cold one by radiation, the copper plate was covered by a 1 mm thick high quality aluminium plate; the thermal contact between these two plates was ensured

Notation

g	Gravitational acceleration
Gr	Grashof number $\equiv g\beta\,(T_p - T_g)H^3\nu^{-2}$
H	Distance between transfer plates
l	Aspect ratio $\equiv L/H$
L	Enclosure dimension in the X-direction
m	Lateral aspect ratio $\equiv M/H$
M	Enclosure dimension in the Z-direction
Pr	Prandtl number
Ra	Rayleigh number $\equiv Gr\ Pr$
Ra_c	Critical Ra number of convection establishment for $\alpha = 0°$
T	Mean temperature $\equiv (T_p + T_g)/2$
T_a	Ambient room temperature
T_g	Cold plate (glass) temperature
T_p	Hot plate temperature
X	Direction along transfer walls and normal to the enclosure rotation axis
Y	Direction normal to the transfer walls
Z	Direction along the enclosure rotation axis
α	Tilt angle
β	Thermal expansion coefficient $\equiv T^{-1}$
γ	Stratification parameter
ν	Kinematic viscosity at T

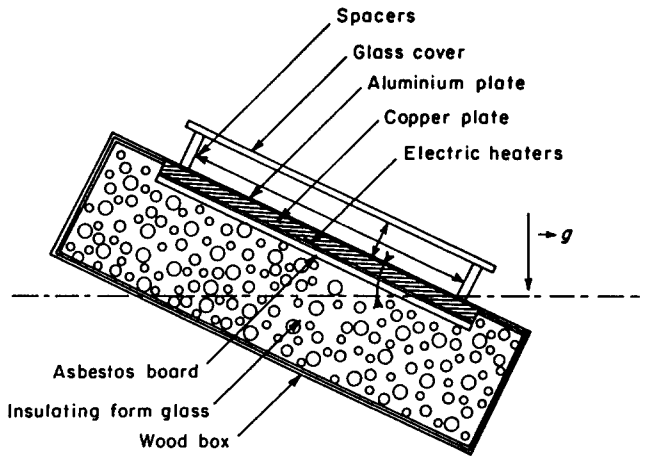

Fig 1 Schematic diagram of the experimental apparatus

by a thin layer of conductive grease in which 15 thermocouples were embedded and uniformly distributed. Inside the useful area of the hot plate, these thermocouples revealed a maximum temperature variation of 1 K over the surface of the plate heated at a temperature of 150°C. Nevertheless, the temperature of the plate was systematically measured during each test and the arithmetic average of the 15 values was taken as the hot plate temperature T_p.

The cold plate consisted of a 5 mm thick glass 0.80 m by 0.80 m thermally free so that its temperature was imposed by the internal flow. Such an unusual condition was chosen because the initial purpose of studying convection motion in this model was in connection with a solar energy flat plate collector and, in particular, the influence of a thermally free cold plate on the internal movements and the heat transfer with respect to a cold plate at an arbitrary temperature. The difficulty in such a model is the measurement of the glass temperature, effected by means of 24 copper–constantan thermocouples fixed at the internal surface of the glass along the plate axis normal to the rotation axis of the model. The small thickness of the thermocouple wires (0.1 mm diameter) is supposed not to affect the internal flow; nevertheless, no other axis was explored because of the disturbance risk of an excessive plot of wires at the glass surface. As a consequence it was assumed that the glass temperature distribution was uniform along the Z-direction: this hypothesis was confirmed by an infrared thermograph of the whole external surface, except for the neighbourhood of the lateral walls of the cavity, where the temperature decreased because of the higher conductive lateral heat transfer. The mean glass temperature $\bar{T}_g$ for evaluating the Rayleigh number was determined as the average

$$\frac{1}{L}\int_0^L T_g(x)\,dx$$

The output voltage of the thermocouples, with the cold source in the melting ice, was recorded with a precision potentiometer. The precision of these temperature measurements, including melting ice temperature, thermocouples tables and potentiometer, was evaluated as ± 0.1 K.

The thickness of the enclosure was varied between 10 mm and 70 mm and maintained constant to within ± 0.2 mm by using four interchangeable end spacers made of 10 mm thick wood. One of the spacers was movable to allow the variation of the L dimension and, therefore, of the aspect ratio L/H for a given value of H. The heater part of the model was mounted in an open insulating wood box 1.15 m by 1.15 m by 0.45 m thick. The inclination angle α of the test enclosure was measured along the glass plate by means of an artillery level to an accuracy of $\pm 0.01°$. The experiments were carried out in a room with the ambient temperature T_a maintained at $22°C \pm 1°C$.

The free convection patterns were visualized by introducing tobacco smoke at two points through holes in the Z-direction lower spacer. Lighting was by means of a 15 mW Spectra-Physics Helium–Neon laser with the beam diverging to a plane sector through a cyclindrical lens (4 mm usual diameter); by turning the lens the orientation of the illuminating sector could be changed from the Z-direction to the X-direction. Exposure times had to be the shortest possible to give the best instantaneous picture of the flow but were typically 1/15 s to 1 s because of the weakness of the laser light. Photographs and viewing were possible through the cover glass of the cold plate.

The establishment of different motion regimes is essentially characterized by the appearance of either steady or unsteady instability. The vertical position of the enclosure, for which the flow is assumed to be two-dimensional, is the simpler case for undertaking such a study. From the results of Bergholz[34] and Thomas and de Vahl Davis[31], it appears that the magnitude of the stable vertical stratification has a strong influence upon the type and character of the instability: this consideration provided the motive for the choice of the X-axis at $Y = H/2$ and $Z = M/2$ to measure the temperature amid the working fluid. These measurements were made by a copper–constantan thermocouple suspended in the fluid by the wires themselves (0.1 mm diameter) passing through slightly oversized holes in the opposite wood spacers; the junction between the two wires was made by electrical contact, so that the solder was of a nearly spherical form close to 0.2 mm in diameter. The displacement of the thermocouple junction was possible by turning the loop made by the two tight wires wound around four pulleys outside the enclosure.

The unsteadiness criterion was based on the immersed thermocouple response. The output was monitored by a printing potentiometric recorder. If the temperature remained constant with time at any point on the X-axis the flow was considered to be steady. Conversely, if the temperature fluctuated anywhere along the X-axis the flow state was considered to be unsteady.

Experimental results and discussion

Lateral aspect ratio effect

The lateral aspect ratio $m = M/H$ is not a fundamental parameter able to affect the flow characteristics, so its effect has received very little attention; generally, authors free themselves of its effect by choosing values sufficiently large to be regarded as effectively infinite and justifying the assumption of two-dimensional motion.

However, some authors have shown that the lateral aspect ratio can have a destabilizing or a stabilizing effect on the onset of a phenomenon. Catton[49],

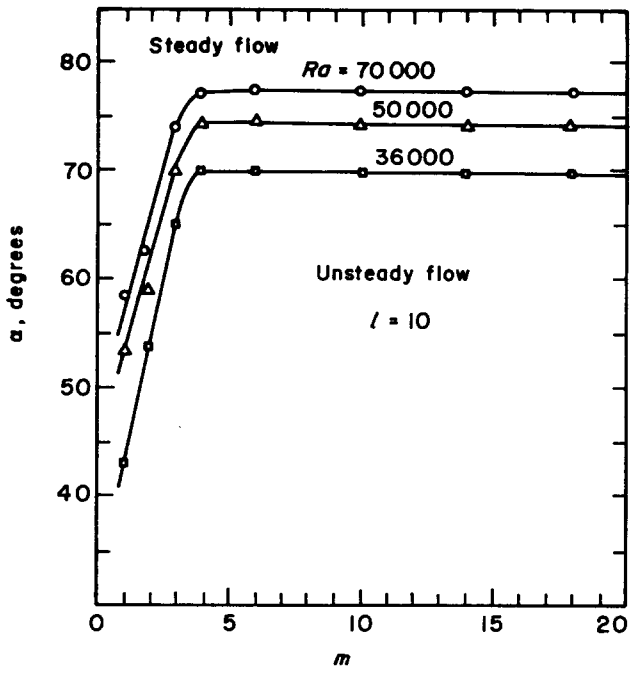

Fig 2 Lateral aspect ratio effect on steady flow limit

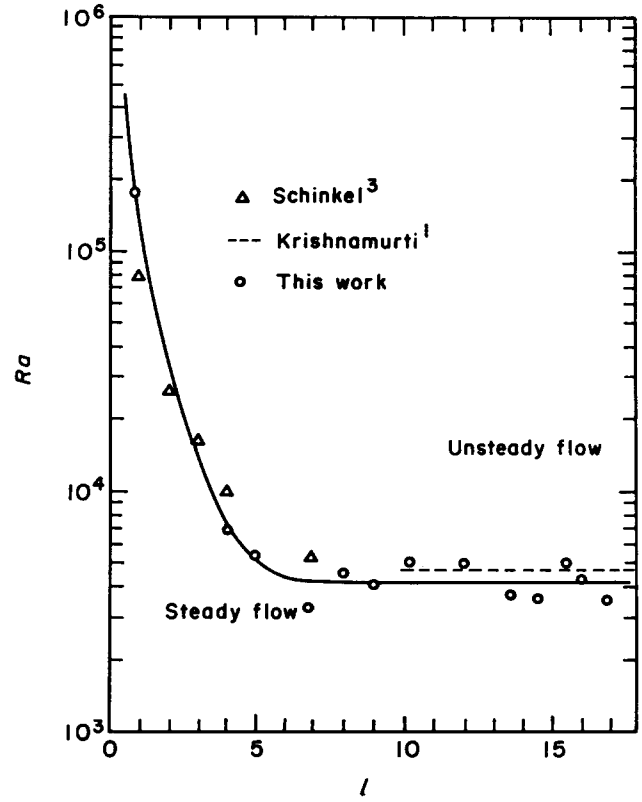

Fig 3 Steady flow for horizontal case ($\alpha = 0$)

then Stork and Müller[50] have pointed out the importance of this parameter in the transition from a conductive regime to a convective one. Their results are in good agreement with the theory of Davis[51] and indicate that its effect cannot be neglected if its value is less that 4. In the case of a vertical cavity, Mallinson and de Vahl Davis[37] have shown a noticeable influence of small aspect ratio ($m < 5$) on three-dimensional effects and heat transfer.

As the present apparatus made possible the variation of the lateral aspect ratio, it appeared interesting to investigate its effect on the limits of steady state of the flow with respect to the tilt angle and the Rayleigh number. The longitudinal aspect ratio was fixed at 10, and the *Ra* value was slowly increased by means of the temperature drop across the fluid layer for a given value of m and α up to the appearance of oscillations of the temperature within the fluid. The experiment was repeated for different values of m from 1 to 18 and different values of α from 0° to 90°.

The data so obtained show a delaying effect of decreasing lateral aspect ratio, ie for a given value of tilt angle the critical value of *Ra* at which the flow becomes unsteady increases with decreasing value of m. The results are presented in Fig 2 in the form of the critical tilt angle versus lateral aspect ratio for some given values of Rayleigh number. It can be observed that the influence of m is noticeable up to a value close to 5, corroborating previous results. Following these results, the experiments described below were carried out for a lateral aspect ratio fixed at 10.

Results for horizontal case

The influence of the aspect ratio on the transition point to time dependence has not yet clearly been studied in the previous works. Krishnamurti[1] pointed out the occurrence of such an influence and found the transition *Ra* value for air to be 2.8 $Ra_c = 4800$* from thermocouple indication and 2.3 $Ra_c = 3930$ from heat flux measurements. These values are given in Fig 3, which shows the critical curve representing the plot of aspect ratio against Rayleigh number. The critical value of *Ra* seems to be independent of l provided it remains greater than 5. The average value of *Ra*, close to 4400 within a maximum deviation of 10%, is found to be in good agreement with those of Krishnamurti. For smaller values of l the critical Rayleigh number increases rapidly with decreasing l, in good agreement with Schinkel's data[3] in spite of a different investigation method; indeed, his unsteadiness criterion was based on flow visualization. It appears, gathering the two types of results, that a limiting value of the aspect ratio can exist below which the flow is stationary for all *Ra* values considered; the present results show that a transition point is found for $l = 0.8$, and Schinkel showed that no transition point was found for $l = 0.50$ or $l = 0.25$. Nevertheless, this hypothesis has to be confirmed by further experiments, for the wall thermal properties are of the first importance in such a study.

The unsteady flow cannot be described, because of the chaotic aspect whatever direction of the laser-plane may be considered. When the motion was stationary, rolls were observed parallel to one another and to the shorter side of the fluid layer, but depending on the mean *Ra* value the flow configuration was quite different in the central part of the cavity from that in the neighbourhood of the side walls; this is caused by the bending of the glass cover so that the width is slightly smaller in the central part and/or by the decrease of temperature owing to the

* Ra_c is the universal critical Rayleigh number from which the free convection begins to occur in a horizontal cavity differentially heated ($Ra_c = 1708$)

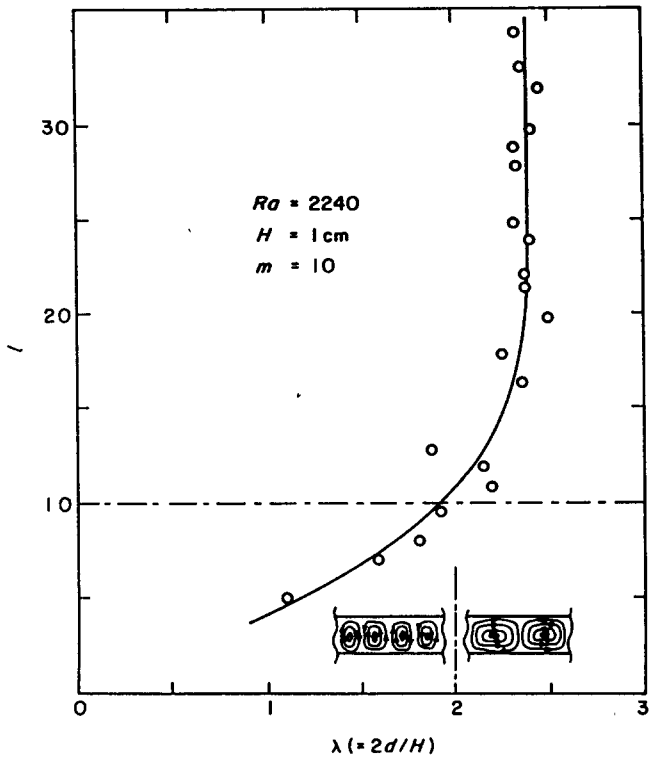

Fig 4 Aspect ratio effect on wavelength ($\alpha=0$)

heat losses through the side walls. That structure is quite similar to the observations of previous experimentalists, particulary Willis and Deardorff[2]. For an Ra value of 2240 the roll size was measured with varying aspect ratio, the thickness H of the fluid layer being fixed at 10 mm. The wavelength equal to twice the width of one roll divided by the cavity thickness is related to the wave number δ by $\lambda\delta=2\pi$. The results given in Fig 4 show that the wavelength increases with l up to nearly 20 and beyond that value up to at least $l=35$, and λ achieves an asymptotic value close to 2.39, in good agreement with the result of Willis *et al*[53] ($\lambda=2.34$ for $l=31.5$). In addition, it is interesting to note the good agreement of the present values of λ versus Ra with the results reported by Willis *et al*[53].

Results for vertical case

All the studies devoted to the determination of the first appearance of instability in a vertical enclosure agree in describing it as transversal rolls with their axis in the Z-direction superposed to the base flow of the conductive regime. For high values of the aspect ratio ($l>20$) this multicellular flow occurs for a fixed Ra value higher than a critical value Ra_{ci} which is slightly different according to different authors, eg 6200[36], 5600[18], 5800[39], 7700[54], 7800[43].

More generally, the diagram (Gr, l) of Roux *et al*[36] gives the theoretical representation of the various types of flow (the Grashof number is more appropriate to the stability analysis at low values of Pr, the disturbances being predominantly shear driven rather than buoyancy driven). This diagram, reproduced in Fig 5, fixes the boundaries of three regions: in region 1 the flow is unicellular, in region 2 transversal rolls appear, and in region 3 the motion becomes unsteady.

The present results concern essentially the boundary between the steady and unsteady states of the flow in the (Gr, l) plane but, as an indication, for $l=13$ the critical Gr value beyond which the flow became unstable was found to be near 10 560, in fairly good agreement with the numerical value close to 9400. When Gr is less than this value, the flow develops in two layers moving upward along the warmer wall and downward along the cooler one. With increasing Gr, viscosity forces become stronger, causing the formation of disturbances in the form of transveral rolls, as shown by the photograph of Fig 6 for $l=13$ and $Gr=10\,600$ in the lower part of the cavity. It is interesting to note that the size of the rolls is noticeably dependent upon the Z position of the sectional view-plane of the flow, which is an indication of the 3D character of the flow. With further increasing Gr values up to about 13 500, the size of the initial steady rolls begins to oscillate with time; then the oscillation magnitude increases until the rolls alternatively vanish and appear again. From a Gr value close to 25 300, the flow becomes again steady and stable with unicellular structure. This reverse transition was indicated by Roux *et al*[36] for $Gr\approx 24\,800$, in very good agreement with the present result. The main characteristic of the present results is the limited range of Gr for which the flow is unstable and stationary (10 560 to 13 500), unlike the numerical prediction (9500 to 25 000).

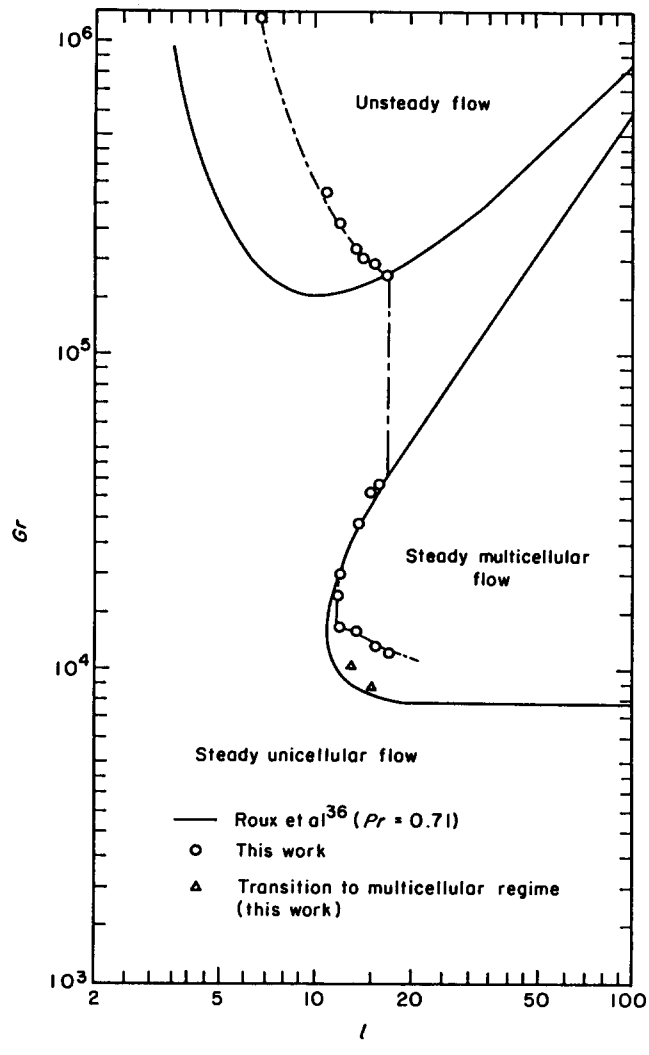

Fig 5 Regimes of motion for vertical case

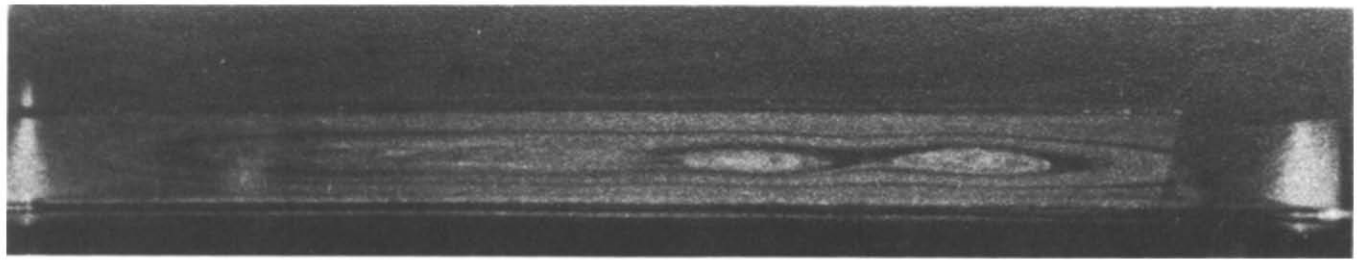

Fig 6 Cross-sectional view of multicellular motion; $\alpha = 90°$, Ra $= 7500$, $l = 13$

In addition, the measurement of the local temperature along the cavity axis shows a slightly linear evolution with the X coordinate except inside the core of the transversal rolls, where the temperature is constant as can be seen from the numerical results of Grondin[44].

Concerning the transition curve from stationary to non-stationary flow in the plane (Gr, l), the first part, relating to the low Gr values, follows the separating curve from region 1 to region 2 of Roux's diagram, so the critical Gr value in the range 40 000–185 000 is independent of the aspect ratio, which keeps a constant value close to 17; this means that, whatever the Gr value may be, the flow is steady for any value of l less than 17 and unsteady otherwise. For Gr values higher than 185 000, the critical value increases with decreasing aspect ratio, following a curve essentially different from the numerically predicted curve; indeed, for a given value of l, the present experiments permitted us to observe a steady flow up to a Gr value higher by one order of magnitude than the predicted value.

These results can be examined in the light of the stability analysis of Bergholz[34], who takes the effect of stratification into account by way of the stratification parameter γ related to the vertical temperature gradient in the cavity by

$$\gamma = \left(\frac{1}{4}\left(\frac{\partial T}{\partial X}\right)\frac{H}{\Delta T}Ra\right)^{0.25}$$

Bergholz's diagram (Ra, γ) reproduced in Fig 7 shows a region I connected to the presence of transverse rolls, a region II characterizing the stable unicellular flow, and a region III relative to the appearance of travelling waves. The present results are plotted for different values of l and show a noticeable effect of this parameter, chiefly for the smallest values. For the highest aspect ratio values and for the low l values, the transition curves approach the Bergholz limit of the stable flow, which is consistent with the previous comparisons; with increasing l, the present transition curve to unsteady flow surrounds the theoretical curve which is established for an infinite fluid layer. Schinkel *et al*[55] have compared their computational results for occurrence of secondary motion with respect to the aspect ratio with the diagram of Bergholz; an obvious similarity with the present results can be observed, although their computations were carried out with stationary equations. Regarding the dimensionless vertical temperature gradient $\tau = (\partial T/\partial X)(H/\Delta T)$, it is interesting to note the fairly good agreement of the present results with the numerical ones of Refs 31 and 36 in the form of τl versus $Ral^{-1.25}$.

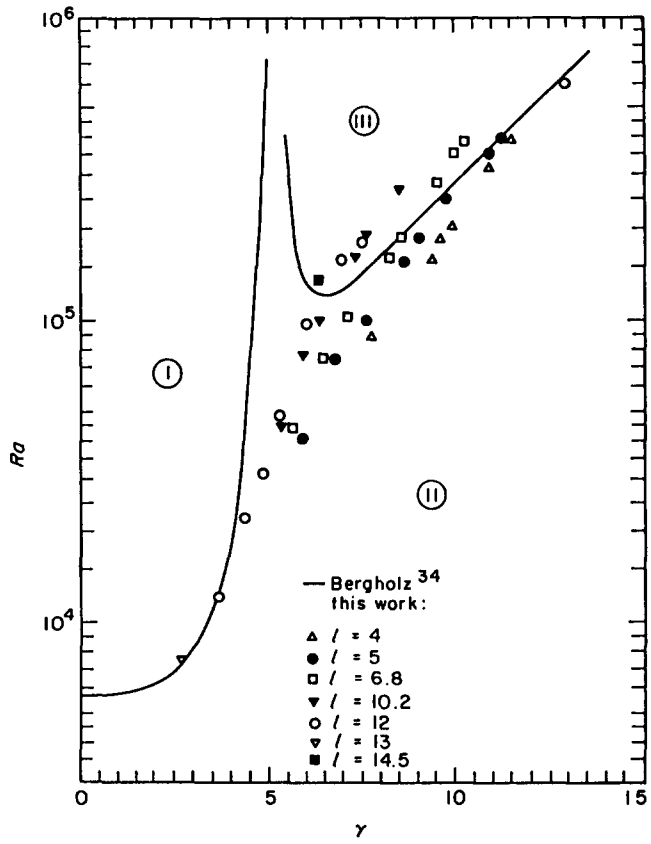

Fig 7 Critical Ra *value versus stratification parameter* ($\alpha = 90°$)

Results for tilted situation

Since the tilt angle is easy to vary, the study of the transition point to unsteady flow was conducted by varying the tilt angle instead of the Ra value through temperature difference. Indeed, the thermal conditions need a long time to be established, and when they are fixed the critical values of tilt angle for fixed l can be determined with good precision within the following ranges: $10^3 < Ra < 10^6$, $3 < l < 17$ and $0° < \alpha < 90°$.

The results are shown in Fig 8 in the form of the critical value of l versus Ra for various values of tilt angle. The diagram indicates a critical tilt angle value, close to 60°, which separates the plane (l, Ra) into two regions. Up to this angle the critical aspect ratio decreases with increasing Ra, and from this angle up to the vertical case the aspect ratio first decreases with Ra to a minimum value for $Ra \approx 10^4$, increases to a maximum value for an

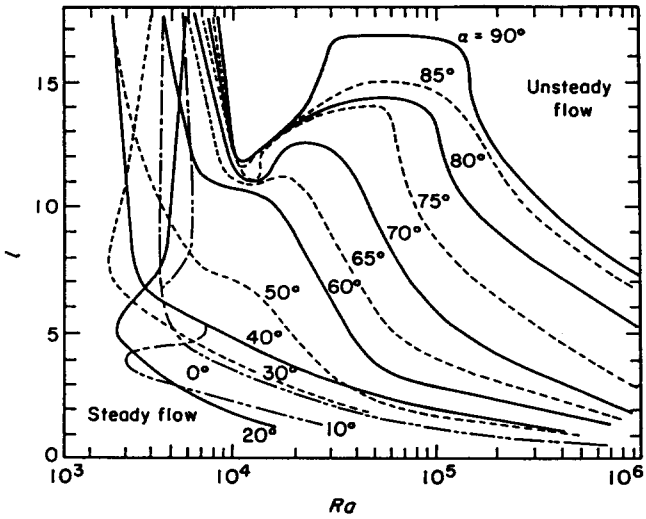

Fig 8 Transition curves (l *versus* Ra) *from steady to unsteady flow for various values of tilt angle*

Ra value which is a function of the tilt angle, and then decreases again. That means a reverse transition of non-stationary to stationary flow for a value of l in the range[11-17] and for a value of α higher than 60°.

Such a result leads to the hypothesis that the flow, which can be assumed to be two-dimensional for the vertical position of the cavity, keeps that two-dimensional character with decreasing tilt angle but with decreasing prevalence, and cancels out for critical value close to 60°; below that value, the flow has to be considered essentially three-dimensional. This assertion is supported by the visual observations in the YZ plane; indeed, for $\alpha = 90°$, and more so for smaller inclinations, a discernible flow appears in close proximity to the walls (about 4% of the cavity depth) turning around the primary cell and giving a third component to the global flow. With decreasing tilt angle, this flow continues to grow in intensity and space so that the 2D character decreases. As the transition from stationary to non-stationary flow sets in more easily in a 3D flow, it is not surprising that, for a given aspect ratio, the critical *Ra* value decreases with decreasing inclination angle.

According to various authors, the critical tilt angle below which the flow cannot be considered as two-dimensional lies between 60° and 70°: Hart[39], Unny[43] and Hollands and Konicek[54] have proposed 70° for high values of l, and Grondin[44] proposed 65° for $l = 16$. For smaller values of l, the structure of the flow remains similar to that developing in the vertical cavity when the boundary layer regime is established; this can be observed through visualization. When the steadiness limit is achieved, the flow moving close to the wall becomes faster and induces disturbance in the streamlines joining the secondary and tertiary cells at each rotation; these disturbances spread to the cells and bring about their time-dependent deformation. Below the critical tilt angle, the process is accelerated, the core is visualized as very diffuse smoke, and the measured temperature fluctuations are quite similar to turbulence.

For a very small aspect ratio ($l = 1$, $H = 5$ cm, $Ra = 3.3 \times 10^5$) the flow remains similar from 90° to 60° with two rolls centred on the normal section diagonal inside the base flow. For smaller tilt angle, the rolls cancel out but the unicellular flow is still in movement; but for $\alpha \approx 60°$ a strange flow is observed, looking like small cells of roughly spherical form (their cross-section by laser plane in any direction has a constant diameter of about 8 to 10 mm). These cells are regularly spaced by a distance close to 50 mm (that is, the cavity depth) along the centre line of the cavity in the Z-direction. Such a flow structure has not previously been identified but it compares to the results of the 3D numerical analysis of Mallinson and de Vahl Davis[37] in a similar geometry, which exhibits the superposition of the axial flow on the cross-sectional flow, looking like the present visualizations.

The vertical case excepted, Schinkel's data[3] provide the only source of comparison, but since the aspect ratio is not higher than 7, even if the two evolution shapes of critical *Ra* value with tilt angle are similar, the order of magnitude of the values is quite different, especially for the high inclinations (the *Ra* values would be lower according to Schinkel) and for small inclinations (the relative values are inverted) as shown in Fig 9. It has to be borne in mind that the unsteadiness criterion is quite different: Schinkel assesses the first non-stationary flow behaviour from the oscillation of the streamlines for a fixed inclination angle from 0° to 90° in increments of 10°,

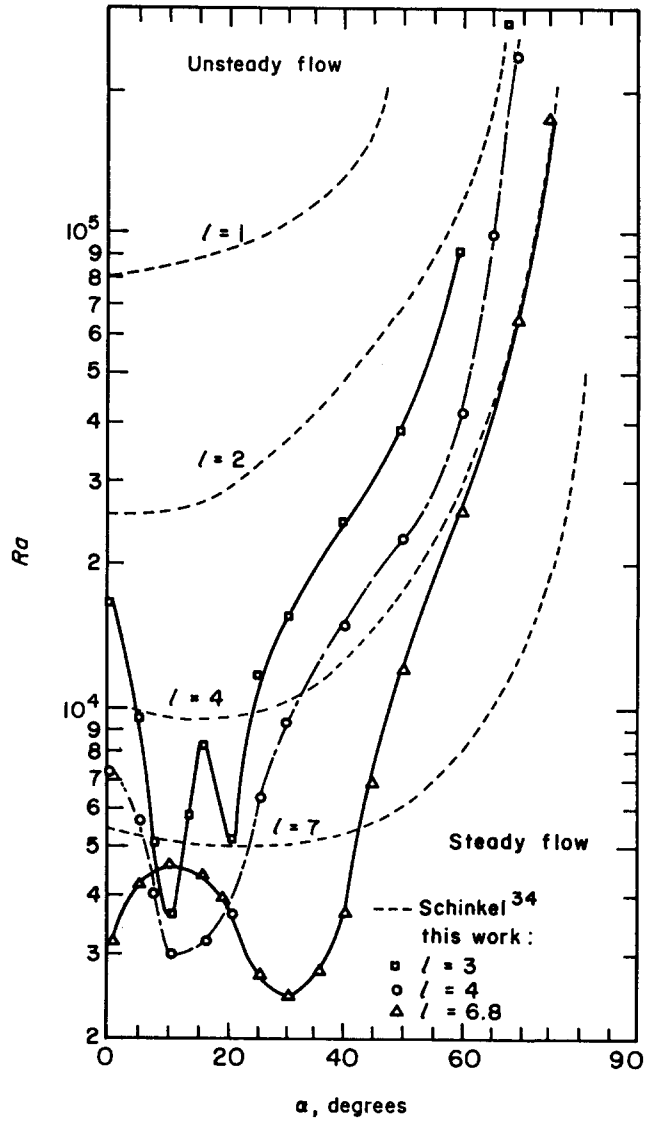

Fig 9 Comparison of present results with Schinkel's data[3] for steady flow limits at low aspect ratios

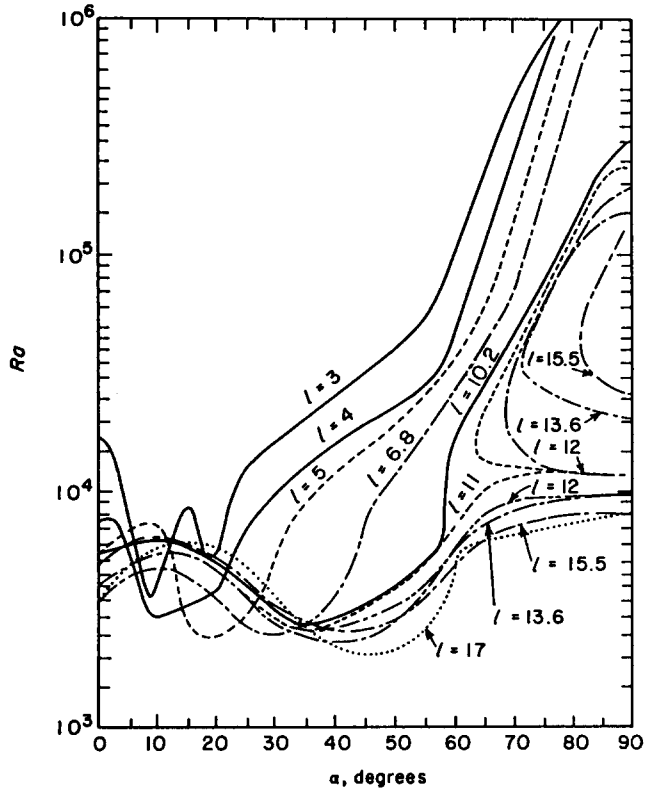

Fig 10 Transition curves (Ra *versus* α) *for various values of aspect ratio*

which is different from the criterion used for this study. In addition, for small tilt angles, Schinkel's curves give food for thought that the critical *Ra* value is constant over an α range which grows wider with increasing aspect ratio. Fig 10 shows *Ra* as a function of tilt angle for different values of aspect ratio. This presentation emphasises the critical value of l close to 11 from which the reverse transition occurs. For aspect ratios less than 11, *Ra* varies non-monotically with α, following a quite sinusoidal evolution for small tilt angles, and then increases with α from a value which increases with l; that increase presents a change of slope for $\alpha_c \approx 60° \pm 5°$ depending on the aspect ratio.

The reverse transition occurs for $11 < l < 17$, and for $\alpha_l < \alpha < 90°$ the limiting value α_l is a function of l. The transition process to unsteady flow occuring for the vertical situation is also appropriate to the slightly less tilted situation for which the angle between the buoyancy field and the velocity field is not too large over the greater portion of the cavity, the end regions excepted, for $l \gg 1$. It appears from visual observations that the flow structure is quite similar for any tilt angle in the range α_l to 90°. Taking into account the role of the space separating the flow near the hot plate from the flow growing along the other plate, about the development of unsteady disturbances, it must be noted that the values of *Ra* relative to a given value of l have been obtained for different values of the thickness, which does not seem to have any effect on the *Ra* values; actually, the visualization shows that the two layers are well separated for any experimental conditions.

According to Elder[38] the first unsteady disturbances, looking like waves, appear near the wall and gradually disrupt the steady cellular pattern in the interior; nevertheless, the co-existence of secondary flows and wall waves is possible. So, it is to be remembered that the present criterion is only relative to the centreline in the X-direction, which means that the present limiting values of stationary flow characteristic parameters are overestimated with respect to the whole flow.

Although the previous theoretical and experimental studies relating to inclined layers did not have exactly the same purpose, it is of interest to compare the present data with their results (for $l = 16$). Fig 11 summarizes the data available in the literature. From Clever and Busse[47] the critical *Ra* value from which stationary longitudinal rolls begin to occur increases with tilt angle according to the law 1708 $(\cos \alpha)^{-1}$. The present visualizations show for $H = 1$ cm, $l = 30$ that this critical *Ra* law gives a good representation of the physical reality up to a tilt angle close to 41°, after which the longitudinal rolls are no longer present. The nearness of the transition curves between $\alpha = 40°$ and $\alpha = 55°$ conveys the idea that the longitudinal rolls become unsteady immediately after their contingent formation. Clever and Busse[47] have proposed also the critical *Ra* value characterizing the onset of the wavy instability for water and air as working fluid. This last instability had been pointed out by Hart[39], whose theoretical and experimental results for water are plotted in the figure.

With respect to the tranverse instabilities, Clever and Busse[47] have proposed their occurrence for a tilt angle close to 71° independent of the *Ra* number up to about 2×10^4, whereas other studies[40,43,44,54] indicate a slight increase of the critical *Ra* value with α up to the vertical situation. Broadly speaking, it appears that the wavy patterns and meanders (as Hart has called them) for $20° < \alpha < 70°$ and the transverse rolls for $70° < \alpha < 90°$ are essentially unstable and their onset just precedes unsteady motions and then turbulence; in addition, this remark seems to be more applicable to a low *Pr* fluid, which is the present case for air.

While looking for the steadiness limits, a wide range of temperature fluctuation types may be observed according to the different parameters. A particular case

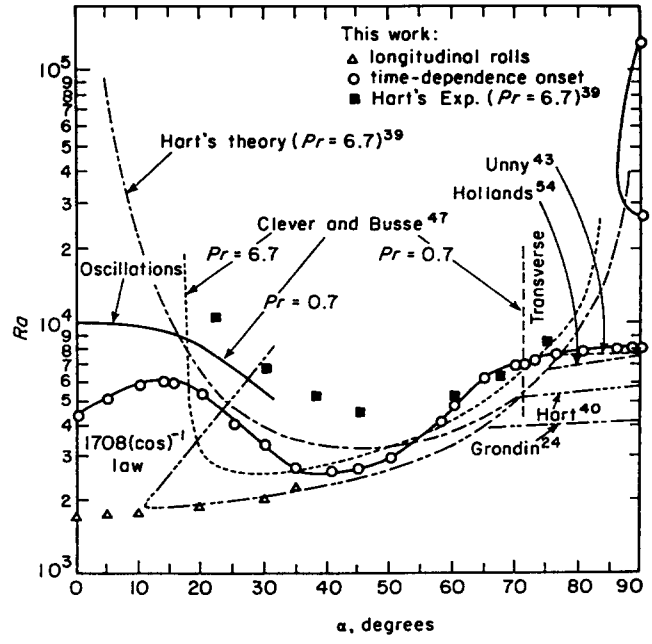

Fig 11 Comparison of transition curves for $l = 16$

($l=8$) has been taken into account with respect to the fluctuations. The discussion is carried out in terms of the Ra values and leads to five regions where the unsteadiness conditions are different with respect to the tilt angle, as follows.

- $Ra<2200$: the flow is stationary for any value of α.
- $2200<Ra<4000$: the temperature is independent of time for small and high values of the tilt angle and is a periodic function of time for a small range of α (for instance, this range runs from 22° to 40° for $Ra=3000$).
- $4000<Ra<6400$: this is the most complex case with five successive states of unsteadiness with increasing α; as an example, the $Ra=5000$ case allows us to identify the following states.

  $0°<\alpha<2°$: the temperature fluctuates in a random manner at a low frequency (about 0.03 Hz).
  $2°<\alpha<19°$: the flow is stabilized, the temperature is stationary.
  $19°<\alpha<30°$: the temperature is subject to periodic oscillations with time.
  $30°<\alpha<48°$: the oscillations of T become of random tupe again but at a higher frequency (about 0.25 Hz).
  $48°<\alpha<90°$: the flow is stabilized again; temperature is constant with time.

- $6400<Ra<9000$: the character of the unsteadiness is similar to the preceding case with the exception that the transition of the low frequency random fluctuations to periodic oscillations occurs directly without returning to the steady state.
- $Ra>9000$: the flow is unsteady over the whole range of α up to the critical value from which the temperature is stationary.

If the temperature oscillation frequency data are collected and plotted versus tilt angle for a given Ra value, increasing frequency is observed with increasing α: the gradient is almost constant when the oscillations are of sinusoidal type, grows noticeably when the oscillations are of any periodic type, and drops abruptly when they become a random type.

These indicative results have given rise to further work to elucidate the correlation between the development and nature of the non-stationary state and the fundamental parameters, Ra value and tilt angle, characterizing the flow structure associated with the aspect ratio.

Concluding remarks

The experimental determination of the transition of a thermal convective flow from a stationary to a non-stationary state in the median part of the cavity brought out the particular complexity of the phenomenon with respect to the three fundamental parameters, Rayleigh number, tilt angle and aspect ratio.

The special situations of the cavity, horizontal and vertical, were considered separately.

For the horizontal position, the stationary limit of the flow was obtained for an Ra value close to 4400 for any aspect ratio greater than 7; for smaller l values, the critical Ra value increased rapidly with decreasing l.

For the vertical position, a plot of the critical Ra value versus aspect ratio followed a curve of a form quite similar to that of stability curves which have been previously obtained numerically. The unstable motions were observed but did not seem to remain stationary for a large range of Ra, and turned rapidly to the time-dependent type. Nevertheless, the reverse transition to the stationary state was actually established.

For the inclined situation, the interdependence as a whole of the three fundamental parameters is presented. The transition curves Ra (l) related to small values of α are fairly similar to those of the horizontal situation, and the transition curves related to high values of α are similar to those of the vertical situation. The limiting tilt angle between the two types of transitional characteristic was found to be close to 60°. The present data have to be completed by a detailed analysis of the different types of time dependence of the flow, as it is shown by the partial results of the present work.

References

1. **Krishnamurti R.** On the transition to turbulent convection. Part 2. The transition to time-dependent flow. *J. Fluid Mech. 1970*, **42**, *309–320*
2. **Willis G. E. and Deardorff J. W.** The oscillatory motions of Rayleigh convection. *J. Fluid Mech. 1970*, **44**, *661–672*
3. **Schinkel W. M. M.** *Natural Convection in Inclined Air Filled Enclosures, Thesis, University of Technology, Delft, The Netherlands, 1980*
4. **Busse F. H.** The stability of finite amplitude cellular convection and its relation to an extremum principle. *J. Fluid Mech., 1967*, **30**, *625–649*
5. **Busse F. H.** The oscillatory instability of convection rolls in a low Prandtl number fluid. *J. Fluid Mech., 1972*, **52**, *97–112*
6. **Busse F. H. and Whitehead J. A.** Instabilities of convection rolls in a high Prandtl number fluid. *J. Fluid Mech., 1971*, **47**, *305–320*
7. **Clever R. M. and Busse F. H.** Transition to time-dependent convection. *J. Fluid. Mech., 1974*, **65**, *625–645*
8. **Batchelor G. K.** Heat transfer by free convection across a closed cavity between vertical boundaries at different temperatures. *Q. Appl. Math., 1954*, **12**, *209–233*
9. **Eckert E. R. G. and Carlson W. O.** Natural convection in an air layer enclosed between two vertical plates with different temperatures. *Int. J. Heat Mass Transfer, 1961*, **2**, *106–120*
10. **Mordchelles-Regnier G. and Kaplan C.** Visualization of natural convection on a plane wall and in a vertical gap by differential interferometry. Transitional and turbulent regimes. *Heat Transfer Fluid Mech. Inst., 1963, 94–111*
11. **Elder J. W.** Laminar free convection in a vertical slot. *J. Fluid Mech., 1965*, **23**, *77–98*
12. **Elder J. W.** Numerical experiments with free convection in a vertical slot. *J. Fluid Mech., 1966*, **24**, *823–843*
13. **Gill A. E.** The boundary layer regime for convection in a rectangular cavity. *J. Fluid Mech., 1966*, **26**, *515–536*
14. **Wilkes J. O. and Churchill S. W.** The finite-difference computation of natural convection in a rectangular enclosure. *AIChE J., 1966*, **12**, *161–166*
15. **de Vahl Davis G.** Laminar natural convection in an enclosed rectangular cavity. *Int. J. Heat Mass Transfer, 1968*, **11**, *1675–1693*
16. **MacGregor R. K. and Emery A. F.** Free convection through vertical plane layers: moderate and high Prandtl number fluids. *J. Heat Transfer, 1969*, **91**, *391–403*
17. **Oshima Y.** Experimental studies of free convection in a rectangular cavity. *J. Phys. Soc. Jpn, 1971*, **30**, *872*

18. **Vest C. M. and Arpaci V. S.** Stability of natural convection in a vertical slot. *J. Fluid Mech., 1969*, **36**, *1–15*

19. **Gershuni G. Z.** Stability of plane convective motion of a liquid. *Zh. Tekn. Fiz., 1953*, **23**, *1838–1844*

20. **Birikh R. V.** On small perturbations of a plane parallel flow with cubic velocity profiles. *Prikl. Mat. Mekh., 1966*, **30**, *356–361*

21. **Rudakov R. N.** On small perturbations of convective motion between vertical parallel planes. *Prikl. Mat. Mekh., 1966*, **30**, *362–368*

22. **Rudakov R. N.** Spectrum of perturbations and stability of convective motion between vertical planes. *Prikl. Mat. Mekh., 1967*, **31**, *376–383*

23. **Gotoh K. and Satoh M.** The stability of a natural convection between two parallel vertical planes. *J. Phys. Soc. Jpn, 1966*, **21**, *542–548*

24. **Gill A. E. and Davey A.** Instabilities of a buoyancy-driven system. *J. Fluid Mech., 1969*, **35**, *775–798*

25. **Gotoh K. and Ikeda N.** Asymptotic solution of the instability problem of channel flows with antisymmetric velocity profile. *J. Phys. Soc. Jpn, 1972*, **32**, *845–850*

26. **Birikh R. V., Gershuni G. Z., Zhukhovitskii E. M. and Rudakov R. N.** On oscillatory instability of plane parallel convective motion of a fluid with a longitudinal temperature gradient. *Prikl. Mat. Mekh., 1972*, **36**, *745–748*

27. **Korpela S. A., Gözüm D. and Baxi C. B.** On the stability of the conduction regime of natural convection in a vertical slot. *Int. J. Heat Mass Transfer, 1973*, **16**, *1683–1690*

28. **Jones I. P.** *Low Prandtl Number Free Convection in a Vertical Slot, Report AERE-A 10416, AERE Harwell, Oxfordshire, 1982*

29. **Birikh R. V., Gershuni G. Z., Zhukhovitskii E. M. and Rudakov R. N.** Stability of the steady convective motion of a fluid with a longitudinal temperature gradient. *Prikl. Mat. Mekh., 1969*, **33**, *958–968*

30. **Gotoh K. and Mizushima J.** The stability of convection between two parallel vertical walls. *J. Phys. Soc. Jpn, 1973*, **34**, *1408–1413*

31. **Thomas R. W. and de Vahl Davis G.** Natural convection in annular and rectangular cavities, a numerical study. *Fourth Int. Congr. in Heat Transfer, NC 2–4, Versailles, 1970*

32. **de Vahl Davis G. and Mallinson G. D.** A note on natural convection in a vertical slot. *J. Fluid Mech., 1975*, **72**, *87–93*

33. **Seki N., Fukusako S. and Inaba H.** Visual observation of natural convective flow in a narrow vertical cavity. *J. Fluid Mech., 1978*, **84**, *695–704*

34. **Bergholz R. F.** Instability of steady natural convection in vertical fluid layer. *J. Fluid Mech., 1978*, **84**, *743–768*

35. **Roux B., Grondin J. C., Bontoux P. and Gilly B.** On a high order accurate method for the numerical study of natural convection in a vertical square cavity. *Numerical Heat Transfer, 1978*, **1**, *331–349*

36. **Roux B., Grondin J. C., Bontoux P. and de Vahl Davis G.** Reverse transition from multicellular to monocellular motion in vertical fluid layer. *Phys. Chem. Hydrodynamics 3-PCH-80, Madrid, 1980*

37. **Mallinson G. D. and de Vahl Davis G.** Three-dimensional natural convection in a box: a numerical study. *J. Fluid Mech., 1977*, **83**, *1–31*

38. **Elder J. W.** Turbulent free convection in a vertical slot. *J. Fluid Mech., 1965*, **23**, *99–111*

39. **Hart J. E.** Transition to a wavy vortex regime in convective flow betwen inclined plates. *J. Fluid Mech., 1971*, **48**, *265–271*

40. **Hart J. E.** Stability of the flow on a differentially heated inclined box. *J. Fluid Mech., 1971*, **47**, *547–576*

41. **Korpela S. A.** A study of the effect of Prandtl number on the stability of the conduction in an inclined slot. *Int. J. Heat Mass Transfer, 1975*, **17**, *215–222*

42. **Birikh R. V., Gershuni G. Z., Zhukhovitskii E. M. and Rudakov R. N.** Hydrodynamic and thermal instability of the steady convective flow. *Prikl. Matem. Mekhan., 1968*, **32**(*2*), *246–252*

43. **Unny T. E.** Thermal instability in differentially heated inclined fluid layers. *Trans. ASME, J. Applied Mech., 1972*, **39**, *41–46*

44. **Grondin J. C.** *Contribution à l'Etude de la Convection Naturelle dans un Capteur Solaire Plan, Thèse de Spécialité, UER-IMFM, Université d'Aix-Marseille II, 1978*

45. **Ozoe H., Sayama H. and Churchill S. W.** Natural convection in an inclined rectangular channel at various aspect ratios and angles. Experimental measurements. *Int. J. Heat Mass Transfer, 1975*, **18**, *1425–1431*

46. **Arnold J. N., Catton I. and Edwards D. K.** Experimental investigation of natural convection in inclined rectangular regions of differing aspect ratios. *Trans. ASME, J. Heat Transfer, 1976*, **98**, *67*

47. **Clever R. M. and Busse F. H.** Instabilities of longitudinal convection rolls in an inclined layer. *J. Fluid Mech., 1977*, **81**, *107–127*

48. **Azouni M. A.** Time dependent natural convection in crystal growth systems. *Physico-Chem. Hydrodyn., 1981*, **2**(*4*), *295–309*

49. **Catton I.** Convection in a closed rectangular region: the onset of motion. *Trans. ASME, J. Heat Transfer, 1970*, **C-92**, *186–188*

50. **Stork K. and Müller U.** Convection in boxes. *J. Fluid Mech., 1972*, **54**(*4*), *599–611*

51. **Davis S. H.** Convection in a box linear theory. *J. Fluid Mech., 1967*, **30**, *465–478*

52. **Krishnamurti R.** On the transition to turbulent convection. Part 1. The transition from two- to three-dimensional flow. *J. Fluid Mech., 1970*, **42**(*2*), *295–307*

53. **Willis G. E., Deardorff J. W. and Somerville R. C. J.** Roll diameter dependence in Rayleigh convection and its effect upon the heat flux. *J. Fluid Mech., 1972*, **54**, *351–367*

54. **Hollands K. G. T. and Konicek L.** Experimental study of the stability of differentially heated inclined air layers. *Int. J. Heat Mass Transfer, 1973*, **16**, *1467–1476*

55. **Schinkel W. M. M., Linthorst S. J. M. and Hoogendoorn C. J.** The stratification in natural convection in vertical enclosures. *19th Natl. Heat Transfer Conf., Orlando, Florida, 1980*